

Spin polarization in open quantum dots

M. Evaldsson and I. V. Zozoulenko

Department of Science and Technology (ITN), Linköping University, 601 74 Norrköping, Sweden

(Dated: November 16, 2018)

We investigate coherent transport through open lateral quantum dots using recursive Green's function technique, incorporating exchange-correlation effects within the Density Functional Theory (DFT) in the local spin-density approximation (LSDA). At low electron densities the current is spin-polarized and electron density in the dot shows a strong spin polarization. As the electron density increases the spin polarization in the dot gradually diminishes. These findings are consistent with available experimental observations. Results of our DFT-based modeling indicate that utilization of the simplified approaches that use phenomenological parameters and/or model Hamiltonians might not be always reliable for theoretical predictions as well as interpretations of the experiments.

Introduction. A detailed understanding of spin-related phenomena in quantum systems is necessary for future spintronics applications such as spin filtering devices[1], spin-FETs [2], nonvolatile computer memories [3], etc. Semiconductor quantum wires, dots and antidots defined in a two-dimensional electron gas (2DEG) represent promising systems for the implementation of quantum spintronic devices [4]. In this context, a topical question is whether the spin degeneracy in these structures can be lifted.

Experimental studies indicate the existence of a spontaneous spin polarization at low densities in the 2DEG[5]. The spontaneous spin polarization was suggested as the origin of “0.7-structure” in the conductance of a quantum points contact (QPC) [6]. Concerning spin polarization in open quantum dots, i.e., dots with strong coupling to leads as opposed to the Coulomb blockade regime, the existing experiments show conflicting findings. A statistical analysis of conductance fluctuations [7] indicated a spin degeneracy at low magnetic fields. The similar conclusion follows from the results of Folk *et al.*[8] who experimentally demonstrated the operation of an open dot as a spin filter. In contrast, low-field magnetoconductance of small dots [9] showed a pronounced peak splitting that was taken as a signature of the spin polarization. In contrast to QPCs, where theoretical investigations of the spin polarization have been a subject of lively discussions during recent years[10, 11, 12, 13, 14, 15], theoretical description of spin-polarization effects in open quantum dots has received far less attention. The main purpose of this paper is to provide such the description.

Modelling transport through quantum dots can be done from conceptually different standpoints. For example, charging and coupling constants might be taken as phenomenological parameters of the theory within a model Hamiltonian [9, 16]. It is however not always evident whether such a simplified description is sufficient to capture the essential physics, and it is not always straightforward to relate quantitatively the above parameters to the physical processes they represent in the real system. Another common approach is to approximate the open system at hand (which is described

by the extended (scattering) states), by a corresponding closed system, and then to calculate a self-consistent potential of this system. The calculated potential is then used to obtain the transmission coefficient on the basis of e.g. transfer matrix technique or related methods[17, 18]. This approach avoids ambiguity related to the choice of a model Hamiltonian and phenomenological constants but depends on the crucial (and not obvious) assumption that there is no qualitative difference between many-electron effective potentials for open and closed systems.

In the present paper we present an approach based on full quantum mechanical many-electron magnetotransport calculations for *open* system. Using the recursive Green's function technique [19] we compute the scattering solutions of the two-dimensional Schrödinger equation in a magnetic field. Following the parametrization for the exchange and correlation energy functionals of Tanatar and Cerperly [20], the electron-electron interaction is incorporated within the Density Functional Theory (DFT) in the Local Spin Density Approximation (LSDA). The choice of DFT+LSDA for the description of many-electron effects is motivated, on one hand, by its efficiency in practical implementation within a standard Kohn-Sham formalism[21], and, on the other hand, by the excellent agreement between the DFT and exact diagonalization[22] and variational Monte-Carlo calculations[23, 24] performed for few-electron quantum dots .

We stress that our approach involves no phenomenological parameters (like coupling/charging constants), and that the self-consistent potential is computed for the scattering states of an open system. As a note, conceptually similar approaches have been used to model quantum transport in molecular conductance and related molecular systems [25] as well as to study quantum point contacts in zero magnetic field[13, 14].

Model. We consider a two dimensional (2D) lateral quantum dot defined by a top gate in a rectangular geometry. The gates induce an external electrostatic confinement described by a harmonic potential [24, 26]

$$v_{ext}(\mathbf{r}) = \frac{1}{2}m^*(\omega_x^2 x^2 + \omega_y^2 y^2). \quad (1)$$

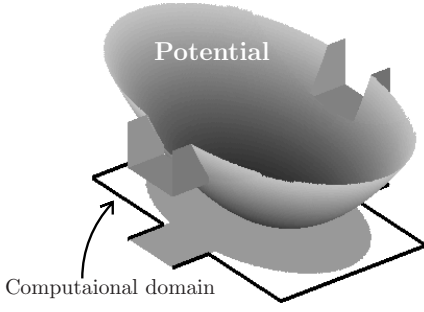


FIG. 1: External confinement potential v_{ext} and the computational area used for the dot. The strength of the confinement is $\hbar\omega_x = 0.2meV$, $\hbar\omega_y = 0.15meV$, the area size is $360 \times 210nm$ and the lead width is $80nm$. Shaded area in the computational domain indicates schematically the region where the confining potential lies below the Fermi level.

The dot is connected to electron reservoirs by two semi-infinite leads, Fig. 1. The total confining potential includes also a contribution from a positive background due to a uniform layer of donors [13]. By changing the donor concentration ρ_+ , which contributes to the classical Hartree potential (Eq. 5), we can effectively alter the electron density in the dot. In this manner, the transport characteristics of dots containing different electron densities can be investigated. In the present paper we present a case study of the magnetotransport in a dot with “low”, “intermediate” and “high” electron densities. This corresponds to a donor concentration $\rho_+/10^{14}m^{-2} = 2, 8, 20$ (resulting in similar average electron densities, \bar{n}_s). The interaction parameter $r_s = 1/a_B^* \sqrt{\pi \bar{n}_s}$, where a_B^* is the effective Bohr radius, is 3.75, 2.00 and 1.28 respectively.

The dot is described by the effective Hamiltonian in a perpendicular magnetic field, $\mathbf{B}_\perp = B\hat{z}$,

$$\hat{H}_{QD}^\sigma = H_0 + v_{eff}^\sigma(\mathbf{r}) + g\mu_B B\sigma, \quad (2)$$

where H_0 is

$$H_0 = -\frac{\hbar^2}{2m^*} \left\{ \left(\frac{\partial}{\partial x} - \frac{eiBy}{\hbar} \right)^2 + \frac{\partial^2}{\partial^2 y} \right\}. \quad (3)$$

In Eq. (3) the Landau gauge is chosen, $\mathbf{A} = (-By, 0, 0)$; m^* is the effective mass in GaAs ($= 0.067m_e$). The last term in Eq. (2) accounts for Zeeman energy where $\mu_B = e\hbar/2m_e$ is the Bohr magneton, $\sigma = \pm \frac{1}{2}$ describes spin-up and spin-down states, \uparrow, \downarrow , and g factor of GaAs is $g = -0.44$.

The effective potential, $v_{eff}^\sigma(\mathbf{r})$, follows from the Kohn-Sham theory [21, 24], and consists of three parts,

$$v_{eff}^\sigma(\mathbf{r}) = v_H(\mathbf{r}) + v_{xc}^\sigma(\mathbf{r}) + v_{ext}(\mathbf{r}). \quad (4)$$

$v_H(\mathbf{r})$ is the classical Hartree potential due to the electron density $n(\mathbf{r}) = \sum_\sigma n^\sigma(\mathbf{r})$, and the layer of positive

donors, ρ_+

$$v_H(\mathbf{r}) = \frac{e^2}{4\pi\epsilon_0\epsilon_r} \int d\mathbf{r}' \frac{n(\mathbf{r}') - \rho_+}{|\mathbf{r} - \mathbf{r}'|}. \quad (5)$$

The exchange and correlation potential $v_{xc}(\mathbf{r}) = v_x(\mathbf{r}) + v_c(\mathbf{r})$ in the local spin density approximation reads [21],

$$v_{xc}^\sigma = \frac{d}{dn^\sigma} \left(n^\sigma \epsilon_{xc}(n, \zeta(\mathbf{r})) \right) \quad (6)$$

where $\zeta = \frac{n^\uparrow - n^\downarrow}{n^\uparrow + n^\downarrow}$ is the spin-polarization. For ϵ_{xc} we have used the parametrization of Tanatar and Cerperly [20]; the explicit expressions for $v_x(\mathbf{r})$ and $v_c(\mathbf{r})$ can be found in [27].

The leads are modeled as hard wall potentials where the magnetic field is restricted to zero. This is fully justified in the field interval under consideration ($B \lesssim 0.5$ T), because the distortion of the wave function in the leads due to the effect of magnetic field is negligible. All the results presented here correspond to one propagating mode in the leads.

Calculations. In order to compute the electron density and the conductance of the dot we use the recursive Green’s function technique[19]. We discretize Eq. (2) and introduce the tight-binding Hamiltonian (with the lattice constant of $a = 10$ nm), where the perpendicular magnetic field is included by Peierl’s substitution [28]. Introducing the retarded Green’s function,

$$\mathcal{G}^\sigma = (E - H^\sigma + i\epsilon)^{-1} \quad (7)$$

we compute the density at site \mathbf{r} through [28]

$$n^\sigma(\mathbf{r}) = -\frac{1}{\pi} \int_{-\infty}^{\infty} \text{Im}[\mathcal{G}^\sigma(\mathbf{r}, \mathbf{r}, E)] f(E - E_F) dE, \quad (8)$$

where f is the Fermi-Dirac distribution and E_F is the Fermi energy. Equations (2)–(8) are solved self-consistently for the spin up/down densities. Note that a direct integration along the real axis in Eq. (8) is rather ineffective as its numerical accuracy is not sufficient to achieve convergence of the self-consistent electron density. Because of this, we transform integration contour into the complex plane $\Im(E) > 0$, where the Green’s function is much more smoother. This also allows us to include bound states in the dot, with energies below any propagating mode in the leads. We would like to stress that the Hamiltonian \hat{H}^σ in Eq. (7) (and thus the corresponding Green’s function \mathcal{G}^σ) correspond to an *open* system representing the quantum dots and semi-infinite leads. Using the converged, self-consistent potential, the transmission coefficient T_σ is computed from the Green’s function between the two leads, $T_\sigma(E) \propto \sum_{m,n} \langle \psi_n | \mathcal{G}^\sigma(\mathbf{r}_{L_R}, \mathbf{r}_{L_L}, E) | \psi_m \rangle$, where $\mathbf{r}_{L_{R,L}}$ denotes the coordinate at the right respectively left lead, and $\psi_{n,m}$ the wave functions in the leads[28]. Finally, the conductance $G = \sum_\sigma G_\sigma$ is found from the Landauer formula, $G_\sigma = -\frac{e^2}{h} \int_{-\infty}^{\infty} T_\sigma(E) \frac{\partial f(E - E_F)}{\partial E} dE$.

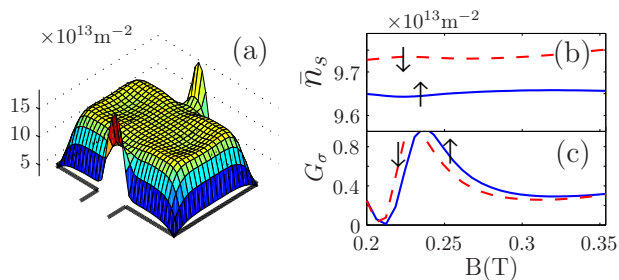


FIG. 2: (color online) (a) The density for the spin-down electrons $n^\downarrow(\mathbf{r})$ in the low density dot calculated within the Hartree approximation (note that $n^\downarrow(\mathbf{r})$ and $n^\uparrow(\mathbf{r})$ are indistinguishable on the scale of figure). (b) Average electron density for spin-down and spin-up electrons in the dot, $\bar{n}_s^\uparrow, \bar{n}_s^\downarrow$ vs. magnetic field. (c) Conductance (in units of e^2/h) through the dot vs. magnetic field. Temperature $T=2\text{K}$.

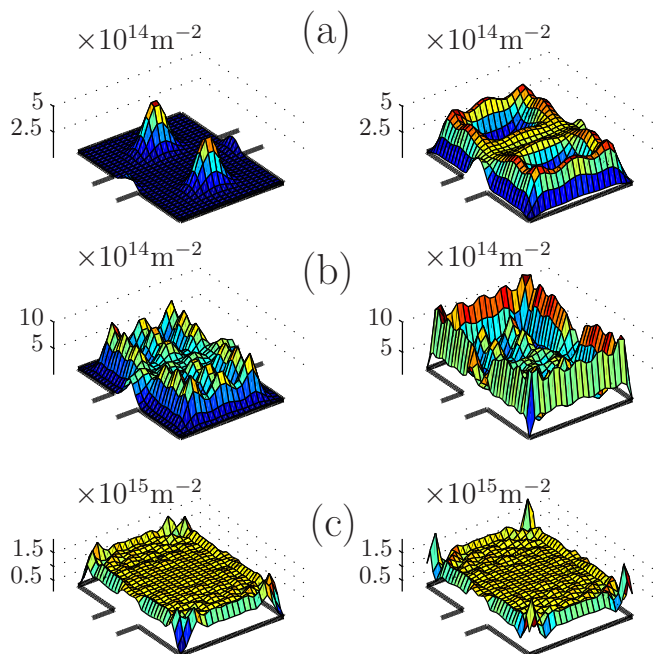


FIG. 3: (color online) The density for the spin-up and spin-down electrons $n^\uparrow(\mathbf{r}), n^\downarrow(\mathbf{r})$ (left and right panels respectively) in a (a) low, (b) intermediate and (c) high density dot calculated within LSDA. $T=2\text{K}$.

Results. To outline the role of exchange and correlation interactions we first study the magnetotransport in a quantum dot within the Hartree approximation (i.e., when $v_{xc}(\mathbf{r})$ is not included in the effective potential (4)). Figure 2(a),(b) show the electron densities $n^\uparrow(\mathbf{r}), n^\downarrow(\mathbf{r})$ and the average spin-up/down density, $\bar{n}_s^\uparrow/\bar{n}_s^\downarrow$, in the low density quantum dot. As expected, the electron densities and the effective potential are practically the same for spin-up/down electrons. Although the Zeeman term lifts the degeneracy between the electrons of different spins, the difference between spin-up/down electrons is very small ($|\bar{n}_s^\downarrow/\bar{n}_s^\uparrow| \sim 1.01$).

Figures 3(a) and 4(a) show the electron densities $n^\uparrow(\mathbf{r}), n^\downarrow(\mathbf{r})$, the average electron densities, $\bar{n}_s^\uparrow, \bar{n}_s^\downarrow$, and the conductance for the small quantum dot calculated in the framework of LSDA, where the effective potential is given by Eq. (4). The difference with the Hartree approximation (Fig. 2) is striking. The exchange interaction causes a significant spin polarization with $|\bar{n}_s^\downarrow/\bar{n}_s^\uparrow| \sim 3$. Note that spin-up and spin-down electrons are spatially separated and localized in different parts of the dot. It is interesting to note that one of the spin channels is completely suppressed such the conductance is dominated by the spin-down electrons. This findings indicate that small quantum dots can be used for injection of the spin-polarized current. It is also important to stress that the spin polarization persists for $B = 0$, which clearly points out to the exchange (not Zeeman) interaction as the origin of the effect.

With the increase of the electron density the spin polarization in the dots decreases. This trend is illustrated in Fig. 4 (b) where the spin polarization in the intermediate density dot is decreased to $|\bar{n}_s^\downarrow/\bar{n}_s^\uparrow| \sim 1.2$, and for the high density dot is practically disappeared $|\bar{n}_s^\downarrow/\bar{n}_s^\uparrow| \sim 1.01$. This behavior is also clearly manifested in the distribution of the electron densities, Fig. 3. In the intermediate density dot the spin-up/down densities $n^\uparrow(\mathbf{r}), n^\downarrow(\mathbf{r})$ are no longer as distinctly separated as in the small one, and in the large dot $n^\uparrow(\mathbf{r}), n^\downarrow(\mathbf{r})$ are, except at the edges, practically the same throughout the dot. The peculiarities at the edges in 3(c) is due to the finite size of our computational domain; as the density and Coulomb interaction increase the electrons are squeezed towards the walls of our confinement. Different electron densities $n^\uparrow(\mathbf{r}), n^\downarrow(\mathbf{r})$ lead to different potentials, which, in turn, result in the difference in the conductance for two spin channels, G_\downarrow, G_\uparrow (Fig. 4, left panel).

The degree of spin polarization in open dots was probed by Folk *et al.* [7] who concluded that the dots were spin degenerate at low field. At the same time, the results of Ref. [9] suggested that the spin degeneracy in open dots is lifted. Our findings reported above seem to reconcile these apparently different experimental observations. Indeed, the dots studied in Ref. [7] had relatively large electron density ($\bar{n}_s \sim 2 \times 10^{15} \text{m}^{-2}$), whereas the dots in Ref. [9] had low electron density, ($\bar{n}_s < 7 \times 10^{14} \text{m}^{-2}$), such that the observed features [7, 9] are consistent with our findings that spin polarization diminishes as the electron density in the dot increases.

During recent years a significant attention has been devoted to the study of the so-called “0.7-anomaly” observed in quantum point contacts (QPCs) [6]. Though still a highly debated issue, this feature has been attributed by many researches to the effect of spin polarization that occurs at low densities when the exchange energy becomes more prominent compared to the kinetic

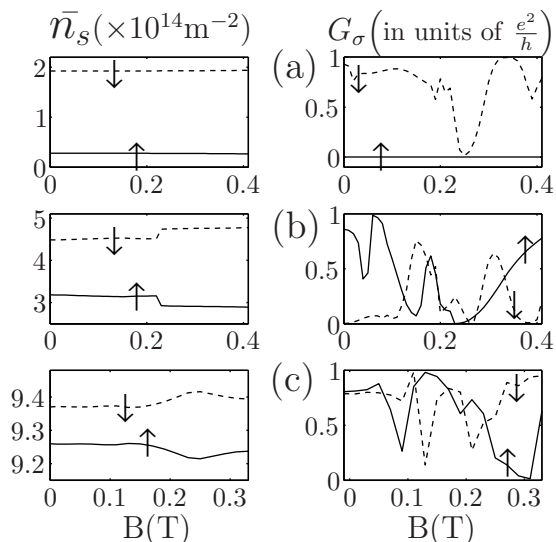


FIG. 4: Average electron density, \bar{n}_s^\uparrow , \bar{n}_s^\downarrow , in the dot (left panel) and conductance (right panel) vs. magnetic field for spin-up and spin-down electrons calculated within LSDA for (a) low, (b) intermediate, (c) high density dots. $B = 0\text{T}$ in (a), (b), and $B = 0.01\text{T}$ in (c). $T=2\text{K}$.

energy [11, 13, 18]. Our present calculations show similar trends in the density dependent spin-polarization in open quantum dots, indicating the similar origin of the effect for these systems. Note that some recent studies question the existence of the spin-polarization in QPCs and attribute the “0.7-anomaly” to different mechanisms, in particular, to the formation of one-dimension (1D) Wigner crystal[15]. Such the interpretation relies on the notion of 1D interacting system. In contrast, our findings strongly indicate that the spin-polarization at low electron densities is a generic feature of both quasi-1D and quasi-0D systems (i.e. QPC and open dots). Because of this, we hope that our results will stimulate further experimental studies of the open quantum dots which might help to settle still unresolved issue concerning the spin polarization in the above systems.

In our previous work [9], we investigated transport in similar dots using the mean-field Hubbard hamiltonian, $H^\sigma = H_0 + U n_\uparrow(\mathbf{r})n_\downarrow(\mathbf{r})$, where on-site Hubbard constant U describes the Coulomb interaction between electrons of opposite spins. Within this model we found that spin polarization in the dot takes place only when the Fermi energy hits the resonant states weakly coupled to the leads. In contrast, the present calculations based on the LSDA shows qualitatively different behavior, when the spin polarization is nearly constant in the broad interval of magnetic field. This difference strongly indicates that utilization of the simplified approaches that use phenomenological parameters and/or model Hamiltonians might not be always reliable for theoretical predictions as well as interpretations of the experiments.

Conclusion. We have performed full quantum mechanical calculations of the magnetotransport in open quantum dots where the electron- and spin interactions have been incorporating within the local spin density approximation. At low electron densities the current is spin-polarized and electron density in the dot shows a strong spin polarization. As the electron density increases the spin polarization in the dot gradually diminishes. These findings are consistent with the existing experimental observations.

Acknowledgements. Financial support from the National Graduate School in Scientific Computing (M.E.) and the Swedish Research Council (M.E. and I.V.Z) is acknowledged. We are thankful to Andrew Sachrajda for discussions and critical reading of the manuscript.

-
- [1] A. Slobodskyy, C. Gould, T. Slobodskyy, C. R. Becker, G. Schmidt, and L. W. Molenkamp, Phys. Rev. Lett. **90**, 246601, (2003)
 - [2] S. Datta and B. Das, Appl. Phys. Lett. **56**, 665 (1990)
 - [3] J. M. Daughton, Thin Solid Films **216**, 162 (1992)
 - [4] G. Burkard, D. Loss, and D. P. DiVincenzo, Phys. Rev. B **59**, 2070 (1999); P. Recher, E. V. Sukhorukov, and D. Loss, Phys. Rev. Lett. **85**, 1962 (2000); I. V. Zozoulenko and M. Evaldsson, Appl. Phys. Lett. **85**, 3136 (2004).
 - [5] A. Ghosh, C. J. B. Ford, M. Pepper, H. E. Beere, and D. A. Ritchie, Phys. Rev. Lett. **92**, 116601 (2004)
 - [6] K. J. Thomas, J. T. Nicholls, M. Y. Simmons, M. Pepper, D. R. Mace, and D. A. Ritchie, Phys. Rev. Lett. **77**, 135 (1996)
 - [7] J. A. Folk, S. R. Patel, K. M. Birnbaum, C. M. Marcus, C. I. Duruöz and J. S. Harris, Jr., Phys. Rev. Lett. **86**, 2102 (2001).
 - [8] J. A. Folk, R. M. Potok, C. M. Marcus, and V. Umansky, Science **299**, 679 (2003).
 - [9] M. Evaldsson, I. V. Zozoulenko, M. Ciorga, P. Zawadzki and A. S. Sachrajda, Europhys. Lett. **68**, 261 (2004)
 - [10] V. V. Flambaum and M. Yu. Kuchiev, Phys. Rev. B **61**, R7869 (2000)
 - [11] C.-K. Wang and K.-F. Berggren, Phys. Rev. B **54**, R14 257 (1996)
 - [12] K. Hirose and N. S. Wingreen, Phys. Rev. B **64**, 073305 (2001)
 - [13] P. Havu, V. Havu, M. J. Puska, and R. M. Nieminen, Phys. Rev. B **69**, 115325 (2004)
 - [14] K. Hirose, Y. Meir and N. S. Wingreen, Phys. Rev. Lett. **90**, 026804 (2003)
 - [15] K. A. Matveev, Phys. Rev. B **70**, 245319 (2004).
 - [16] A. Groshev, T. Ivanov, and V. Valtchinov, Phys. Rev. Lett. **66**, 1082 (1991); C. Niu, L.-J. Liu, and T.H. Lin, Phys. Rev. B **51**, 5130 (1995); B. R. Bulka and P. Stefański, Phys. Rev. Lett. **86**, 5128 (2001)
 - [17] D. Jovanovic and J.-P. Leburton, Phys. Rev. B **49**, 7474 (1994); Y. Wang, J. Wang, H. Guo and E. Zaremba, Phys. Rev. B **52**, 2738 (1995)
 - [18] K.-F. Berggren and I. I. Yakimenko, Phys. Rev. B **66**, 085323 (2002);
 - [19] F. Sols, M. Macucci, U. Ravaioli, and K. Hess, J. Appl.

- Phys. **66**, 3892 (1989)
- [20] B. Tanatar and D. M. Ceperley, Phys. Rev. B **39**, 5005, (1989)
- [21] R. G. Parr and W. Yang, *Density-Functional Theory of Atoms and Molecules*, (Oxford Science Publications, Oxford, 1989).
- [22] M. Ferconi and G. Vignale, Phys. Rev. B **50**, R14722 (1994).
- [23] E. Räsänen, H. Saarikoski, V. N. Stavrou, A. Harju, M. J. Puska, and R. M. Nieminen, Phys. Rev B **67**, 235307 (2003).
- [24] S. M. Reimann and M. Manninen, Rev. Mod. Phys. **74**, 1283 (2002)
- [25] P. S. Damle, A. W. Ghosh, and S. Datta, Phys. Rev. B **64**, 201403(R) (2001); J. Taylor, H. Guo and J. Wang, Phys. Rev. B **63**, 245407 (2001)
- [26] A. Kumar, S. E. Laux and F. Stern, Phys. Rev. B, **42**, 5166 (1990)
- [27] M. Macucci, Karl Hess and G.J. Iafrate, Phys. Rev. B **48**, 17354 (1993)
- [28] S. Datta, *Electronic Transport in Mesoscopic Systems*, (Cambridge University Press, Cambridge, 1997)